Renewable Energy 187 (2022) 34–43

Contents lists available at ScienceDirect

Renewable Energy

journal homepage: www.elsevier.com/locate/renene

Bio-inspired bistable piezoelectric energy harvester for powering animal telemetry tags: Conceptual design and preliminary experimental validation

Feng Qian [a, b], Mingyi Liu [a], Jianuo Huang [a], Jiajun Zhang [a], Hyunjun Jung [c], Zhiqun Daniel Deng [a, c], Muhammad R. Hajj [d], Lei Zuo [a, c, *]

[a] Department of Mechanical Engineering, Virginia Tech, Blacksburg, VA, 24061, USA
[b] Department of Mechanical Engineering Technology, Pennsylvania State University, the Behrend College, Erie, PA, 16563, USA
[c] Energy and Environment Directorate, Pacific Northwest National Laboratory, Richland, WA, USA
[d] Department of Civil, Environmental and Ocean Engineering, Stevens Institute of Technology, 1 Castle Point Terrace, Hoboken, NJ, 07030, USA

ARTICLE INFO

Article history:
Received 21 April 2021
Received in revised form
30 November 2021
Accepted 5 January 2022
Available online 15 January 2022

Keywords:
Piezoelectric
Energy harvesting
Bio-inspired
Bistable vibration
Telemetry tag
Animal tracking

ABSTRACT

This paper presents the conceptual design, preliminary experimental validation, and performance evaluation of a novel bio-inspired bi-stable piezoelectric energy harvester for self-powered animal telemetry tags. The overall conceptual design, which includes a bio-inspired attachment and a bi-stable piezoelectric energy harvester, is introduced firstly with a specific application example of marine fish tracking. The self-powered telemetry tag can be externally deployed on fish (dorsal fin) to monitor fish habitats, population, and underwater environment. Inspired by the Venus flytrap's rapid shape transition, a bi-stable piezoelectric energy harvester is developed to scavenge energy from fish maneuvering and the surrounding fluid flow for a sustainable power supply. The bistability of the harvester is characterized by the measured force-displacement curve and double potential wells. A bluff body is integrated to the free end of the bistable piezoelectric energy harvester to enhance the structure-fluid interaction for the large-amplitude snap-through vibrations and higher voltage output. Controlled laboratory experiments are conducted in a water tank on the bio-inspired bi-stable piezoelectric energy harvester using a servo motor system to simulate fish swing motion at various conditions to evaluate the power generation performance. The preliminary underwater experimental results demonstrated that the proposed bio-inspired bi-stable piezoelectric energy harvester could effectively convert fish swing motions into electricity. The device collected 17.25 mJ of energy over 130 s under a peak-to-peak swing angle of 30^{o} at 1.5 Hz in the capacitor charging experiments.

© 2022 Elsevier Ltd. All rights reserved.

1. Introduction

The fast development of wireless sensor networks has enabled the long-term, automatic, continuous, and simultaneous tracking of wild animals whose habitats range from the poles to the tropics and the photic zone to the abyssal depths [1,2]. The data collected from tracked animals provides unprecedented insight into the ecology, such as animal migration patterns, problems posed by invasive species and spread of zoonotic diseases, animal-environment interactions, population declination due to land-use changes. The information could also then significantly benefit natural conservation and resource management. One specific example is fish tracking which has been recognized as one effective way to evaluate the impacts of marine hydrokinetic energy technologies, offshore wind energy farms, and hydroelectric power stations on animal passage and mitigation [3]. The primary tool for remotely tracking fish is the acoustic telemetry tag which transmits a unique acoustic signal to multiple local receivers (hydrophones) that extract the arrival time and identification code from the acoustic waveform [4]. The tagged fish could be then located from the processed data based on the time-difference-of-arrival (TDOA) algorithm in three dimensions [5]. Fish tags can be categorized into surgically implanted ones and externally deployed ones depending on the targeted animals [6]. The external attachment method was

* Corresponding author. Department of Mechanical Engineering, Virginia Tech, Blacksburg, VA, 24061, USA.
E-mail address: leizuo@vt.edu (L. Zuo).

https://doi.org/10.1016/j.renene.2022.01.018
0960-1481/© 2022 Elsevier Ltd. All rights reserved.

the most commonly used method in the initial applications (1956–1975), later, it was overtaken by surgical implantation due to the tag miniaturization and extended battery life [6]. Recently, the external deployment method has increased with the development of archival tags (data storage tags, DSTs), pop-up satellite archival tags (PSATs), and other environment-sensing tags. These fish tags are mostly powered by batteries that require periodic replacement due to the limited energy capacity and could cause potential chemical contamination to the marine ecosystem. For example, the Vemco V16 tag is powered by a lithium-ion battery, which will corrode over time and the plastic tag casing might rupture, leading to lithium leaching [7]. The limited power supply constrains the tracking and communication distances and has been a major bottleneck that hinders the widespread applications of acoustic animal telemetry tags. Periodic battery replacements are expensive, harmful to animal growth and survival, and even impossible in practice due to the far distance migration of marine animals.

One possible solution to the above-mentioned issue is to harvest energy from the surrounding ambient and animal motions to provide continuous, reliable, and sufficient power for fish tags. In practice, the externally deployed fish tags are usually subjected to multiple excitation, including fish maneuver, fluid flow, and random disturbance over a broadband frequency range. Integrating proper transducers to fish tags can convert this kinetic energy into useable electricity and enable self-powered fish tags, which could operate without solely relying on traditional batteries and thus elongates the service life and the life of the tagged fish. A comprehensive study on the lifetime and power consumption of marine tag technologies and the potential energy source in the marine environment concluded that harnessing either the fluid flow associated with the swimming animal or the pressure energy could meet the power requirements of current bio-logging systems [8]. Research in energy harvesting from fluid and animal motions has explosively increased in recent years. Different energy harvesters have been developed for converting fluid-induced vortex vibrations (VIV) and galloping into electricity [9–11]. A bionic-fin-inspired triboelectric nanogenerator was developed to harvest water-flow for powering real-time undersea detection [12]. A piezoelectric beam energy harvester was used to gather energy from a flying pigeon. It produced 0.1 mW power which is in the order of the power requirements of the microcontrollers used in bio-logging applications [13]. Energy harvesting from fish swimming using ionic polymer-metal composites (IPMCs) [14] and piezoelectric macro fiber composite (MFC) transducers have been experimentally demonstrated based on a biomimetic fishtail for underwater temperature sensing, and wireless data transmission [15]. The piezoelectric fish-like bimorph cantilevers with a passive caudal fin (tail) were experimentally studied for underwater power generation [16]. A self-powered fish tag was developed using a flexible piezoelectric beam to harvest the mechanical energy from the fish body during swimming [17]. This is the first known implantable energy-harvesting fish tag demonstrated in vivo, which could send a unique identification code for a detection range of up to 100 m. However, the linear piezoelectric beam harvester worked at a very low frequency (off-resonance) during fish moving, leading to a very small power output of 14 μW due to the frequency mismatch [18].

As for the linear piezoelectric energy harvesters that have been widely studied, high power can only be attained at the resonant vibration, and therefore the frequency bandwidth is limited [19], as a result of which a slight frequency mismatch could lead to significant power reduction [18,20]. Fish motion, fluid flow, and other random disturbance in the marine environment have a wide range of frequency components and various uncertainties, which constitute broadband frequency excitation to the harvester. Any mismatch between the natural frequency of the harvester and excitation frequency leads to a significant drop in the power output. These facts require that the harvester be able to scavenge energy effectively over a wide frequency range. Nonlinearity has been widely recognized as an effective mechanism to extend the frequency bandwidth of vibration energy harvesters [21–23]. Nonlinear vibration systems typically have bending frequency curves and therefore could achieve large-amplitude vibrations over a wide range of excitation frequency. Bi-stable nonlinear harvesters can achieve better performance than their linear counterparts because the snap-through dynamics, also referred to as the global vibration, could lead to large-amplitude vibrations and thus high voltage output [24–26]. Research has shown that multiple excitation and random disturbance could enhance the power output of bistable harvester by promoting the snap-through vibrations [27,28]. Therefore, bistable piezoelectric energy harvesters are more favorable for self-powered fish tag applications since the multiple excitation frequencies from fish swimming, fluid flow, and random disturbance could increase the probability of the large-amplitude snap-through vibrations, thus, higher power output over a broad range of excitation than linear responses.

This paper presents the conceptual design and preliminary experimental demonstration of a bio-inspired bistable piezoelectric energy harvester to achieve an autonomous power supply for continuous fish tracking by harvesting energy from fish maneuvering and surrounding fluid. The overall conceptual design of the self-powered fish telemetry tag is firstly introduced and the bio-inspired design of the bistable piezoelectric energy harvester is briefly described. The bistability of the harvester was characterized by measuring the force-displacement curves and the potential function obtained by integrating the fitted force-displacement curves. Underwater experiments were performed in a water tank to demonstrate the feasibility of energy harvesting from fish swing and evaluate the power generation performance of the bio-inspired bistable piezoelectric energy harvester under various load conditions and external electrical resistance. A servo motor driving system was designed to simulate the fish swing during swimming as the base excitation to the harvester. The average power output of the harvester was evaluated at different swing angles and frequencies, as well as the external electrical resistance. The innovations of the paper include: 1) concept evaluation of a bio-inspired design of the energy harvesting fish tag; 2) development, testing and characterization of a bio-inspired bi-stable piezoelectric energy harvester for underwater applications; 3) experimental study on the snap-through dynamics from swing motions of the bistable piezoelectric energy harvester. The results show that more energy can be attained from the large-amplitude snap through oscillations at a low swing frequency.

2. Bio-inspired design of the self-powered fish telemetry

2.1. Overall conceptual design

The overall design of the self-powered fish telemetry tag should consider the functions, reliability, and environment. The functions include energy harvesting from ambient excitation, sensing, and wireless data transmission. The conceptual design of the proposed self-powered fish tag is illustrated in Fig. 1, which consists of a sucking disc for attachment and a bistable piezoelectric energy harvester with a bluff body. This study mainly focuses on the development of a bistable piezoelectric energy harvester for the self-powered fish tag; therefore, the acoustic transmitter, circuit board, and integrated sensors were not included in Fig. 1 since they are out of the scope of this work. The bluff body is to enhance the

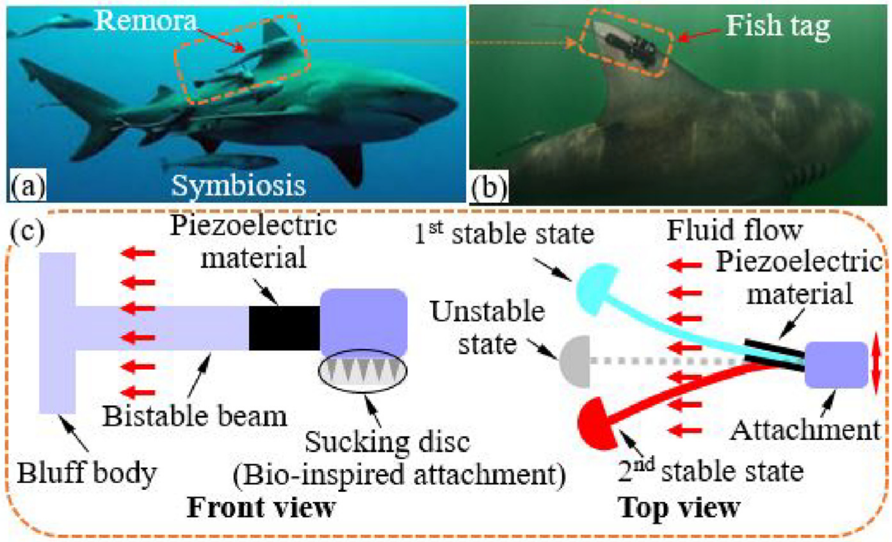

Fig. 1. Bio-inspired design of the self-powered fish telemetry tags: (a)symbiotic relationship between remoras and a shark (b) electronic tag externally deployed on a shark dorsal fin (c) concept design of the attachment and the proposed bi-stable piezoelectric energy harvester with a bluff body for the enhancement of fluid-structure interaction.

harvester's interaction with the surrounding fluid to facilitate the large-amplitude snap-through vibration of the bistable energy harvester. As the fish tag vibrates under the base excitation from fish swing and fluid flow, the piezoelectric element mounted close to the fixed end of the harvester will convert the induced strain into electric charges based on the direct piezoelectric effect [29]. An energy harvesting circuit manages the charges, and a super-capacitor is used to store the harvested electricity, which powers the sensing and data transmission units of the fish tag. Two innovations are proposed in this design. One is the sucking disc attachment method. The other is the bistable piezoelectric energy harvester with the bluff body for energy harvesting from multiple excitation sources. This study focuses on the latter one, but a brief introduction is given to the attachment's conceptual design in the following for a complete picture.

One challenge of fish tracking technologies is how to attach telemetry tags to fish with minimum or without influence on their normal life. Instead of clamping them to the fin or surgically implanting them inside fish bodies, a novel attachment inspired by the symbiotic phenomenon between remoras and sharks is proposed to attach the harvester to fish. As shown in Fig. 1 (a), remoras can attach to a shark by special sucking discs in their mouths. This action is referred to as a symbiotic relationship. It was observed that regardless of the size of the remora fish, it is unlikely that the shark will dislodge a remora by increasing its swimming speed [30]. The remoras' low drag profile and suction-based attachment strategy are the keys for the shark to travel everywhere without paying extra effort. This symbiotic relationship does not influence the shark's movement but benefits both the remoras and the shark. This interesting phenomenon inspired a novel attachment design for fish tagging more efficiently, leading to the concept of replacing the remoras with a smaller and lighter self-powered bio-inspired fish tag. Understanding the mechanism of this process provides new sights in the design of attachable devices. The adhesive disc on the remora's head has a complex mechanism that includes a modified fin structure with teeny spikes (called lamellar spinules) that generate friction to adhere to the host. By learning and mimicking this fin structure with teeny spikes, a bio-inspired attachment sucking pad can be designed for the proposed self-powered fish tag by employing proper materials and structures.

2.2. Bio-inspired bistable piezoelectric energy harvester

The self-powered fish tag needs to provide sufficient power from multiple excitations, including fish swing motion, fluid flow, and random disturbance, under which traditional linear resonant energy harvesters are inefficient due to the frequency mismatch. However, the bistable energy harvester design is quite challenging for the specific application conditions of the underwater marine environment. Existing mechanisms in literature to realize bistabilities mainly include mechanical pre-loading [18,31], magnetic interaction [32,33], and residual thermal stress in laminate composite [34,35]. Both the axially preloaded and magnet-based bistable beam energy harvesters make the system bulky and awkward because redundant constraints are essential for these methods. In comparison, laminate composites are not reliable and stable in an aquatic environment. This study aims to investigate a novel bi-stable piezoelectric energy harvester inspired by the biology phenomenon of Venus flytrap (Dionaea muscipula) to provide a continuous, reliable, and sufficient power solution to externally deployable fish tags. The Venus flytrap is a good example of bi-stable non-linearity in nature which could trap agile insects by quickly closing its two leaves within a very short time (100 ms) [36], as shown in Fig. 2 (a) and (b). A rapid shape transition occurs from the open state (Fig. 2 (a)) to the close state (Fig. 2(b)) when the leaves are triggered to snap shut. This rapid shape transition is referred to as the snap-through of bi-stable structures, usually accompanied by a large energy release.

By studying the structures of the Venus flytrap leaves, which substantially contribute to the bistability of the plant, it is found that the leaves curve and stretch in two directions at the open state and store potential energy in the stretched deformation. The snap-shut motion from the open state to the close state is accompanied by a significant energy release from the leaves. Inspired by the bi-curved shape of the Venus flytrap leaves, a bi-stable piezoelectric energy harvester is designed by pre-stressing two mutually constrained sub-beams that are tailored from a cantilever, as shown in (Fig. 2(c)). The cantilever beam is made of steel and has an overall dimensions of 149 mm × 40 mm × 0.38 mm. The strip of 2.0 mm width at the middle of the cantilever along the length direction is cut off. Then, a piezoelectric macro fiber composite transducer

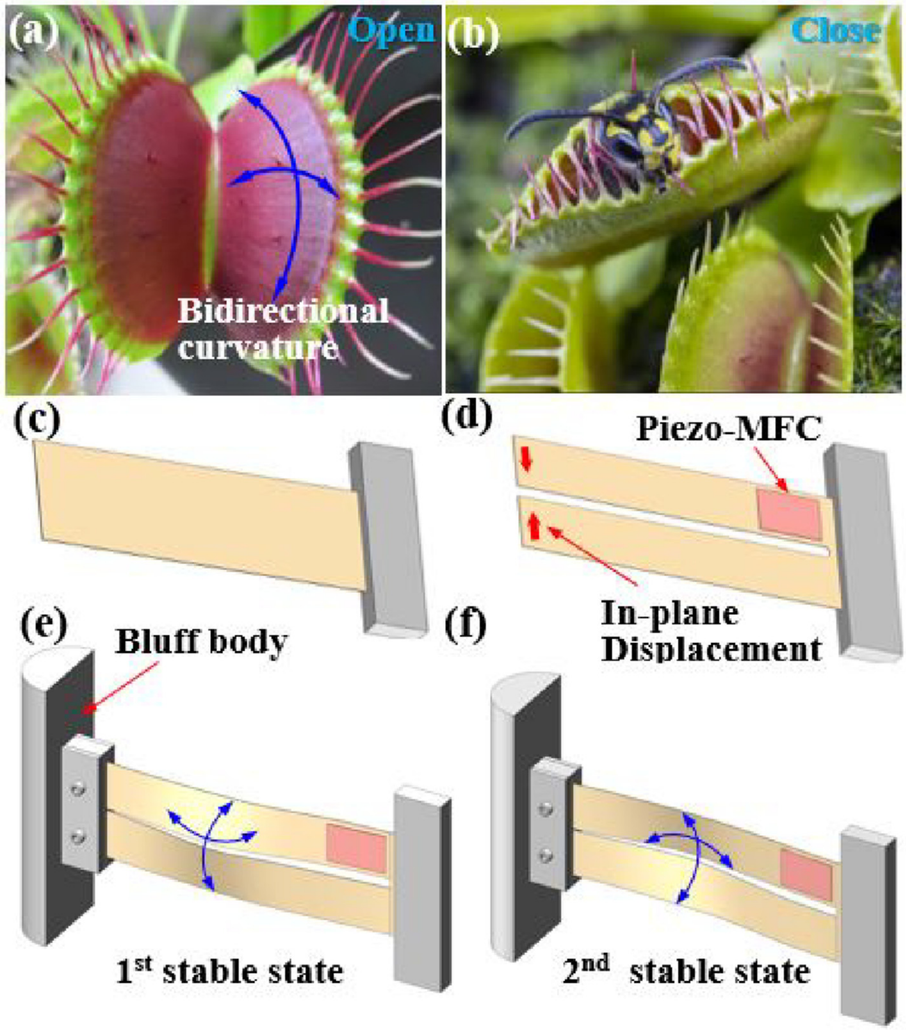

Fig. 2. Bio-inspired design of the bistable piezoelectric energy harvester: (a) open state of the Venus flytrap with the leaves curved in two directions (b) close state of the Venus flytrap (c) cantilever beam (d) tailored cantilever beam with the attached piezoelectric MFC transducer and the applied in-plane displacement constraint at the free ends of the sub-beams (e) first stable state and (f) second stable state of the bio-inspired bistable piezoelectric energy harvester with a bluff body.

(MFC, M2814-P2, Smart Material Corp.) is mounted on the surface of one of the resultant two sub-cantilever beams at the location close to the fixed end. The active length and width of the piezoelectric MFC transducer are 28 mm and 14 mm, respectively. In-plane displacement constraint is then applied to the free ends of the two sub-beams so that the two beams move toward each other at the free ends, as illustrated in (Fig. 2(d)). The in-plane displacement constraint bends and twists the two sub-beams so that the sub-beams are curved in two directions similar to the Venus flytrap leaves and therefore induces mechanical potential energy inside the two sub-beams. The displacement constraint is held by two rigid blocks and screws at the free ends, which also connect the cantilever with the bluff body. Since the bending and twisting deformations are bi-directional, as shown in (Fig.2(e) and (f)), the harvester has two stable states and one unstable state. The detailed design and working principle of the bistable structure are referred to Ref. [37]. The bluff body is added to the harvester's free end to increase the fluid-structure interaction for energy harvesting. As an initial attempt, the dimensions of the bluff body were determined based on the experimental trial, which could enable the snap-through dynamics at the considered excitation conditions. The diameter and length of the bluff body are 40 mm and 100 mm, respectively. The combination of the fluid-induced vibration energy harvesting strategy with bi-stable characteristics creates a new harvester expected to have a much better performance in terms of power generation. When the harvester is integrated into fish tags and deployed on the dorsal fin of fish, it will be subjected to the base excitation from fish swing, ambient fluid flow, and random disturbance. The multiple excitations could benefit the large amplitude inter-well oscillations of the bi-stable harvester, which are desirable for large power output. Compared with other bistable energy harvesters realized by magnetic forces and composite laminates, the proposed harvester is easy to manufacture and does not require a magnetic field. Since the proposed bio-inspired bistable piezoelectric energy harvester does not need additional magnets and is simply made of metal sheet, the cost would be significantly lower than the magnet- and composite laminate-based harvesters.

3. Bistability characterization

The force-displacement curve is measured from experiments to characterize the bistability of the proposed bio-inspired piezoelectric energy harvester. The experimental setup for measuring the force-displacement curve of the harvester is shown in Fig. 3, where the harvester was fixed to a fixture and connected to the force gauge (Mark-10 M2-2) with a U shape adapter and two conical pins inside the adapter. A ball-screw system drives the force gauge on it and, therefore, could push forward and pull backward the harvester's free end to measure the force at different locations. Meanwhile, the electronic digital step gauge rigidly connected with the ball-screw system measures the traveling displacement of the force gauge, which was also the deformation of the harvester at the free end. As the ball-screw system drives the force gauge and the digital step gauge to move forward, the harvester will snap through from one stable state to the other one and vice versa. In this way, the displacement of the harvester at the tip will be measured synchronously together with force, and therefore the force-displacement curve of the harvester could be attained. The potential energy of the harvester could be obtained by integrating the fitted force-displacement curve, from which the bistability could be intuitively observed from the two potential wells and the barrier.

Fig. 4 (a) plots the measured data points of the forces and displacements (star and circle markers) during the force gauge traveled forward and back. The curves are the two fitted fifth-order polynomial models. The two pentagrams at A_0 and C_0 indicate the two equilibrium positions corresponding to the first and second stable states, respectively, where the forces are zero. Fig. 4 shows that the force-displacement curve of the piezoelectric energy harvester is discontinuous, quite different from the continuous one of a typical bi-stable system. This singularity of the force-displacement curve can be attributed to multiple factors, such as the complicated boundary conditions, imperfect geometry properties, and asymmetrical pre-stress distribution in the harvester. The difference between the two sub-beams due to the manufacturing errors would be the main cause. The discrepancy between the sub-beams, particularly the unlike stiffness, makes the mutual constraint and interaction between them more complicated, leads to the asynchronous snap-through motions of the two sub-beams, and creates the asymmetric potential wells, which are definitely worth further exploration in the future. Similar force-displacement curves were also found in other bi-stable systems, such as the bi-stable composite structure [35] and shallow arch [38].

During the experiment, the harvester was first pulled back to position A from the first stable state, and thus the force is negative and then gradually driven forward. The nonlinear restoring force follows the A-A_0-B-B_0 (C-C_0-D-D_0) branch as the force gauge moves

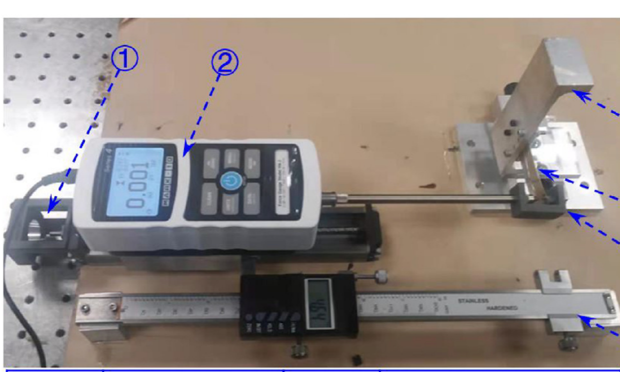

NO.	Component	NO.	Component
①	Ball-screw system	④	Harvester
②	Force gauge	⑤	Adapter
③	Fixture	⑥	Electronic digital step gauge

Fig. 3. Experimental setup for bistability characterization.

forward (backward), which increases along with the displacement and the stiffness is positive, then comes to a maximum at B (D). After that, the force decreases due to the effect of the negative stiffness. At the point B_0(D_0), the sub-beams suddenly jumped from the first stable state to the other stable state because as the displacement keeps on increasing, the work done by the driving force is large enough to overcome the potential energy inside the sub-beams. During this process, the proposed bio-inspired bistable harvester exhibits a hardening stiffness from point A_0 to A (C_0 to C), softening stiffness from point A_0 to B (C_0 to D), and negative stiffness from point B to B_0 (D to D_0). The measured force-displacement explicitly shows the bistability and the stiffness features of a bistable system.

The potential energy of the bio-inspired piezoelectric energy harvester was attained by integrating the fitted polynomial models of the nonlinear restoring forces and plotted in Fig. 4 (b). The results show that the potential of the harvester has two asymmetric potential wells and independent barriers. As mentioned above, the asymmetry in the potential wells is originated from the manufacturing errors of the two sub-beams. The effect of the piezoelectric MFC transducer can also result in the asymmetry in the potential wells. Nevertheless, the two potential wells are clear evidence that categorizes the proposed bio-inspired harvester into the bistable system. The bistable system dynamics significantly depend on the potential plotted in Fig. 4 (b). Generally, the harvester with deeper wells is more likely trapped in one of the potential wells (intra-well vibration) reflected as the small-amplitude local oscillations. This is because deeper potential wells require more energy input to overcome the resultant higher barriers. From the perspective of energy harvesting, the harvester is expected to snap through one potential well to the other, leading to large-amplitude inter-well oscillations and, therefore, higher power output. In such a case, the bistable system with lower potential wells and barriers is more desirable, particularly for weak excitation. Research also showed that the asymmetry in the potential wells degrades the mean power output of bi-stable harvesters subjected to the random excitation of low to moderate noise intensities [27,39].

For the proposed bio-inspired bistable piezoelectric energy harvester, the potential inside the harvester is a function of the in-plane pre-displacement applied at the free ends of the sub-beams. Therefore, the potential of the harvester is tunable by adjusting the pre-displacement constraint. It takes more effort to impose a larger in-plane displacement at the harvester's free ends, but that will result in larger pre-stress and deformations in the sub-beams, which implies more input energy. Therefore the potential wells of the resultant system are deeper. In turn, a smaller in-plane displacement is easier to exert to the free ends but will induce smaller pre-stress and deformations in the sub-beams, which indicates less energy and thus shallower potential wells. Besides, the symmetric potential wells can also be achieved by subtly tailoring the sub-beams.

4. Underwater experimental setup

Experiments are conducted in a water tank to evaluate the energy harvesting performance of the proposed bio-inspired bistable piezoelectric energy harvester based on the simulated underwater fish swing motion. A controlled servo motor system was designed and built to mimic the fish swing motion, which provided the harvester with base excitation. The goal of the experimental studies is to investigate how the swing angle, swing frequency, and electric resistance affect the dynamics and power generation performance of the harvester. The resistance sweep experiments are firstly conducted for two swing angles of 15^o and 30^o (peak-to-peak

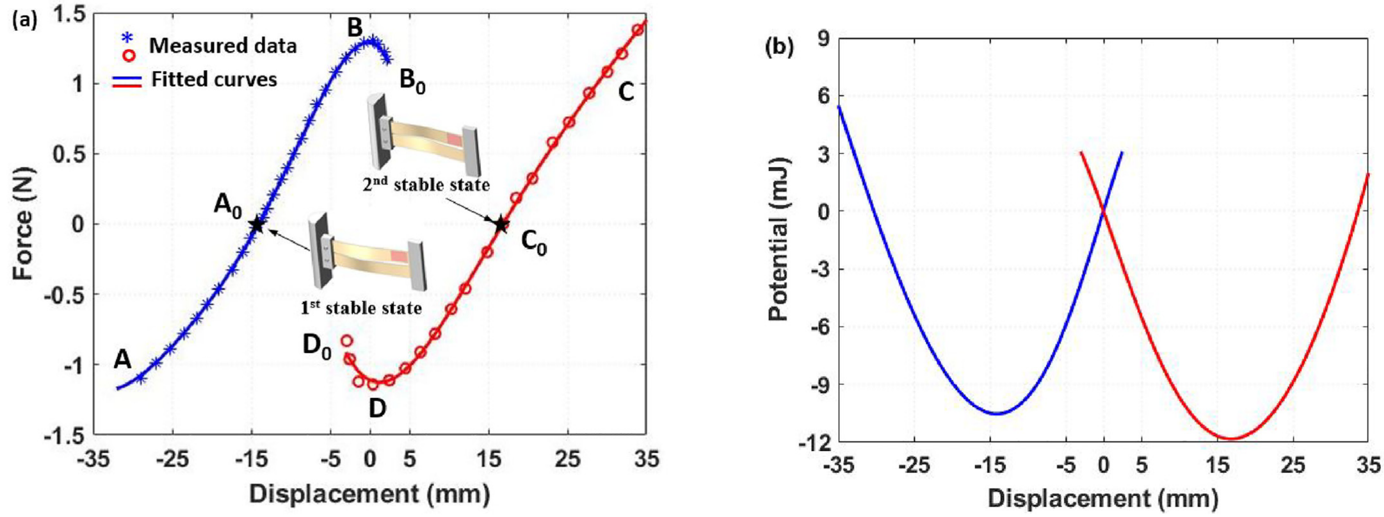

Fig. 4. (a) Force-displacement curves and (b) the potential of the bio-inspired bistable piezoelectric energy harvester.

angle) at constant swing frequencies to identify the optimal resistance corresponding to the maximum power output. Then frequency sweep experiments are also performed at the two swing angles and constant resistance to find the onset frequency of the large-amplitude snap-through vibration and the corresponding average power output of the harvester. The power generation performance of the harvester is investigated at local vibration and global snap-through vibration under different excitation amplitudes and frequencies.

In the experiments, a servo motor (57HSE2.2N + HBS57 Closed-loop step motor) is employed to simulate the fish swing motion that drives the harvester to vibrate through a wood shaft. The overall experimental setup is shown in Fig. 5, where the left part shows the water tank test layout. The servo motor was placed on the top of the tank. The wood shaft was used to transfer the motor rotation to the harvester fixed at the lower end of the shaft. A hollow shaft precision potentiometer (NP32HS) is installed on the output shaft of the motor to measure the rotational angle (swing angle), which is also the base excitation angle of the harvester. A 3D printed U-shape adapter connected the servo motor with the wood shaft to transfer the rotation stably. A bearing at the bottom of the tank is used to hold the wood shaft to keep it stable and aligned with the motor shaft. The swing angle defined in this paper is the peak-to-peak rotation angle of the shaft. The FLEX SEAL (B00L3MDI0I, Swift Response, LLC), a rubberized sealant spray coating, is sparged over the piezoelectric FMC and wires for waterproof in the experiment. The right part of Fig. 5 shows the DC power source, energy harvesting circuit, and the circuits for the entire experiment system control. The servo motor was controlled by the stepping motor drive (HBS57). The excitation angle amplitude and frequency were programmed and fed to the microcontroller (MSP432, Texas Instruments), which controls the servo motor drive. The MASTECH DC power supply (HY3005F-3) is used to power the servo drive, motor, potentiometer, and control circuit. The oscilloscope (Tektronix TDS2014C) is used to display and record the generated voltage of the harvester and the sensor signal.

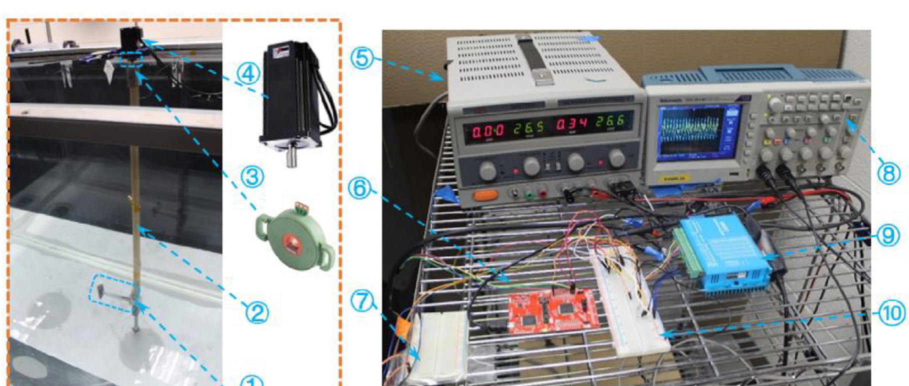

NO.	Component	NO.	Component
①	Harvester	⑥	Micro controller
②	Shaft	⑦	Energy harvesting circuit
③	Angle sensor	⑧	Oscilloscope
④	Servo motor	⑨	Stepping motor drive
⑤	Power supply	⑩	Control circuit

Fig. 5. Underwater experimental setup.

It should be mentioned that the experiments were conducted in still water, which means the fluid flow effects were not considered because of the limited experimental conditions of the small tank. Theoretically, the fluid flow surrounding the harvester could significantly contribute to the power generation and change the nonlinear dynamics of the harvester because of the fluid-structure interaction, such as vovortex-induced vibrations (VIV). The interaction between the fluid flow and the bluff body could facilitate the desired large-amplitude snap-through vibration of the proposed BBPEH. The influence of the water flow velocity, vortex, and the bluff body dimensions on the snap-through dynamics and power generation performance is a very interesting direction to further explore and definitely worth more effort and attention in the future. In addition, turbulent and stochastic flow can also be explored to promote the large-amplitude snap-through vibrations. Further parametric evaluation of flow conditions and performance optimization of the harvester is certainly necessary especially when considering the fish size and swimming conditions.

5. Results and discussion

Different excitation angles and frequencies are considered in the experiments to study the energy harvesting performance of the bio-inspired bistable piezoelectric energy harvester. An electrical resistance sweep was firstly conducted by switching the resistors in the energy harvesting circuit to find the optimal resistance corresponding to the maximum power output at different load conditions. Then frequency sweep was performed to the harvester connected to a selected resistor to investigate the influence of the swing frequency on the dynamics and power output. The sweep frequency range of 0.8–1.6 Hz was considered based on the measured tail-beat frequency of sharks with the body length in the range of 30–121 cm and swimming velocity varying from 20 cm/s to 95 cm/s [40].

Finally, the experimental demonstration was carried out by charging a capacitor with the harvested voltage using a bridge rectifier that consists of four diodes. As an example, Fig. 6 plots the open-circuit voltage output and the potentiometer sensor output for the swing angle of 30° and frequencies of 1.1 Hz and 1.5 Hz. During the experiments, the harvester oscillated around one of the local stable states at the excitation frequency of 1.1 Hz. It snapped through from one stable state to the other at the excitation frequency of 1.5 Hz. The peak-to-peak open circuit voltage output of the harvester at the two excitation frequencies are 80 V and 181 V, respectively, which implies that larger voltage was obtained from the large-amplitude snap-through dynamics of the bistable energy harvester. The sensor output shows the same peak-to-peak rotational angle of the motor.

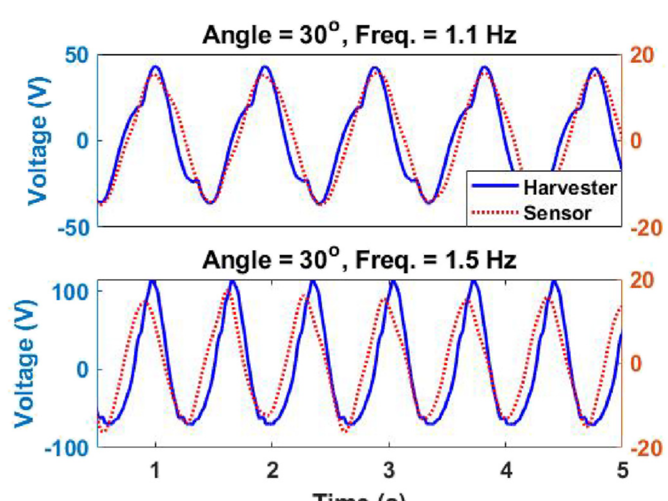

Fig. 6. Open circuit voltage output and sensor output at the swing angle of 30° and frequencies of 1.1 Hz and 1.5 Hz.

5.1. Resistance sweep

The average power output of the harvester over the external resistance can be calculated by

$$P_{avg} = \frac{1}{T}\int_0^T \frac{v(t)^2}{R}\mathrm{d}t. \tag{1}$$

where $v(t)$ is the time series of the voltage output, T is the total time, and R is the external resistance. The average power output of the harvester is presented in Fig. 7 for the varying external resistance under the swing angle of 15° and the swing frequencies of 1.0 Hz and 1.1 Hz. No snap-through dynamics was observed during these experiments because of the small swing angle and lower frequencies. It is found that the harvester followed the shaft rotation and oscillated around one of the stable states. The maximum average power output is very small, which is 0.020 mW and 0.027 mW at the two excitation frequencies. The corresponding optimal resistance at both frequencies is 1.5 MΩ. The average power output of the harvester at the swing angle of 30° and frequencies of 1.0 Hz, 1.1 Hz, and 1.2 Hz is plotted in Fig. 8 (a) versus the varying resistance. The maximum average power at these frequencies is around 0.058 mW, 0.088 mW, and 0.143 mW, and the corresponding optimal resistance is also found to be 1.5 MΩ. Although the large-amplitude snap-through vibrations were still not observed at these excitation frequencies, the average power output is much larger than the one at the swing angle of 15° in Fig. 7 because of the increase in the swing angle.

As the swing frequency increased to 1.3 Hz and 1.5 Hz, the large-amplitude snap-through dynamics was observed, and higher voltage output was obtained. The average power output at the excitation frequencies of 1.3 Hz and 1.5 Hz is plotted in Fig. 8 (b) over different resistance. Compared with the results in Fig. 8 (a), it can be seen that a much larger power output is attained at these two slightly higher frequencies, at which the harvester oscillated from one stable state to the other one. The maximum average power output at the frequencies of 1.3 Hz and 1.5 Hz is 0.70 mW and 1.18 mW, respectively. Another observation is that the optimal

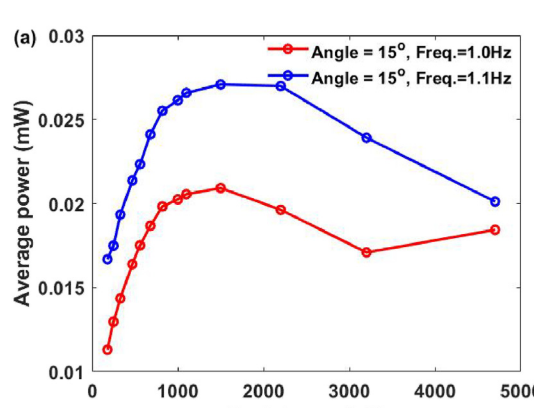

Fig. 7. Average power output at the swing angle of 15° and frequencies of 1.0 Hz and 1.1 Hz.

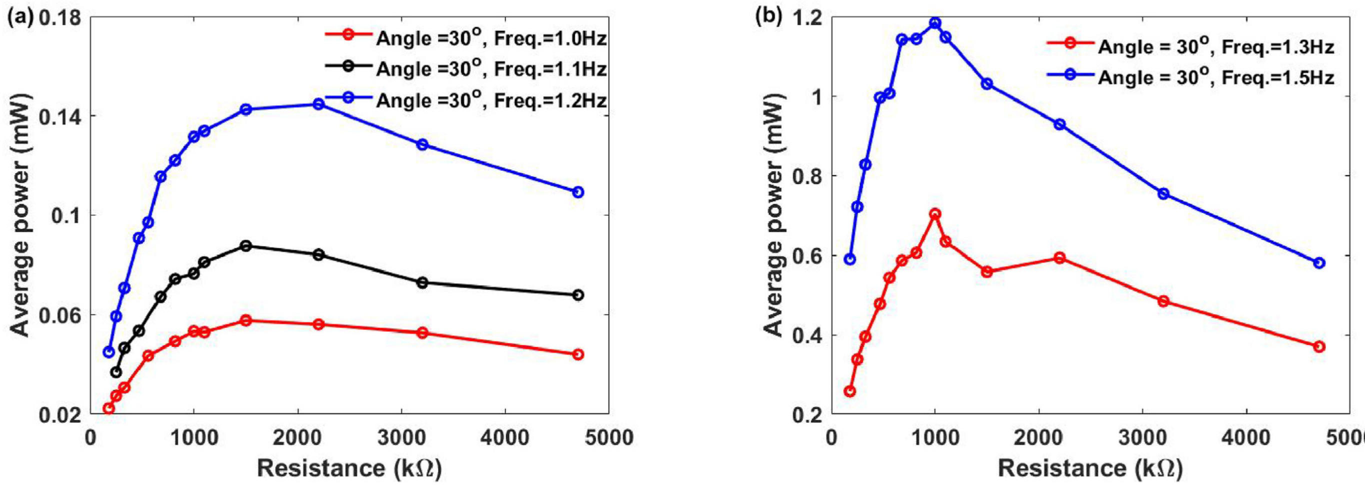

Fig. 8. Average power output of (a) local vibration at the swing angle of 30° and frequencies of 1.0 Hz, 1.1 Hz, and 1.2 Hz (b) global vibration at the swing angle of 30° and frequencies of 1.3 Hz and 1.5 Hz.

resistance corresponding to the maximum power is reduced to 1.0 MΩ compared to the one at lower excitation frequencies. This is because the voltage responses of the bistable piezoelectric energy harvester contain higher frequency components during the snap-through vibrations [37]. The optimal resistance for a piezoelectric energy harvester is related to the capacitance C_p of the transducer, and the vibration frequency ω by [41].

$$R_{opt} = \frac{1}{\omega C_p}. \quad (2)$$

This indicates that the optimal resistance reduces as the vibration frequency of the harvester increases for the given capacitance, which explains the maximum power was obtained at the smaller resistance at the frequencies 1.3 Hz and 1.5 Hz.

5.2. Frequency sweep

To further explore the influence of the swing frequency on the power generation performance, experiments were conducted on the harvester at the varying frequency for the two swing angles of 15° and 30° at the constant external resistance of 1.0 MΩ. This resistance was chosen in the experiments because it's optimal for the case of the large-amplitude global vibration. The average power output of the harvester is presented in Fig. 9 for the two swing angles versus the varying excitation frequency. The results show that for both swing angles, the average power output is very small when the swing frequency is less than 1.2 Hz because the harvester oscillated around one of the local stable states, which resulted in very low voltage output. The onset frequency of the large-amplitude snap-through vibration can be observed from Fig. 9, which is 1.4 Hz for the swing angle of 15° and 1.3 Hz for the swing angle of 30°, respectively. The average power output of the harvester increases quickly along with the swing frequency after the snap-through vibration was activated. The maximum average power output of 1.5 mW was achieved at the swing angle of 30° and frequency of 1.6 Hz. The power density has been widely used in literature to evaluate the power generation performance of energy harvesters with different scales. The power density of 2.4×10^{-2} mW/cm^3 was obtained by normalizing the average power to the total volume of the harvester including the bluff body. It is noted that this result was obtained with the initial design without parameter optimization and fluid flow excitation.

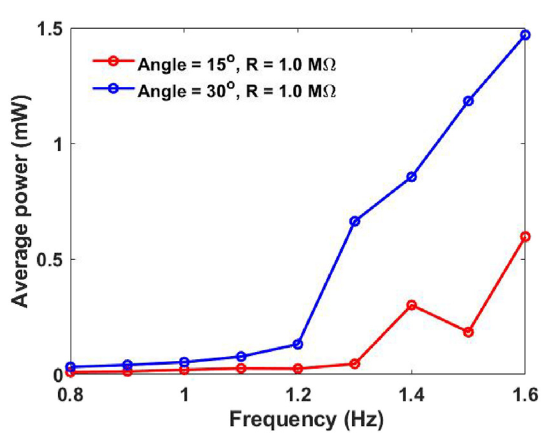

Fig. 9. Average power output over the varying swing frequency at the excitation angles of 15° and 30°.

5.3. Capacitor charging

The harvested irregular voltage must be rectified and stored in a capacitor that powers sensors, circuits, and the data transmission unit to provide sustainable energy for animal telemetry tags. Therefore, it's necessary to demonstrate that the proposed bio-inspired bistable piezoelectric energy harvester could successfully charge a capacitor with the voltage harvested from the underwater swing motion. An AC-DC interface circuit, as illustrated in Fig. 10 (a), was built to convert the AC voltage output of the harvester into DC voltage, which includes a full bridge rectifier. The circuit setup of the capacitor charging tests is shown in Fig. 10 (b), where four Schottky 1 N5817 diodes were used in the full-bridge rectifier and the capacitor of $C_c = 22$ μF was charged in the experiments. The swing angle of 30° and three different swing frequencies of 1.1 Hz, 1.3 Hz, and 1.5 Hz were considered in the tests. The capacitor was fully discharged before each test to study the charging process.

Fig. 11 presents the time evolution of the voltage measured on the capacitor during the charging experiments at the three swing frequencies. It can be seen that the voltage across the capacitor increases firstly and then reaches the maximum values, which are the peak DC voltage output of the full-bridge rectifier at the

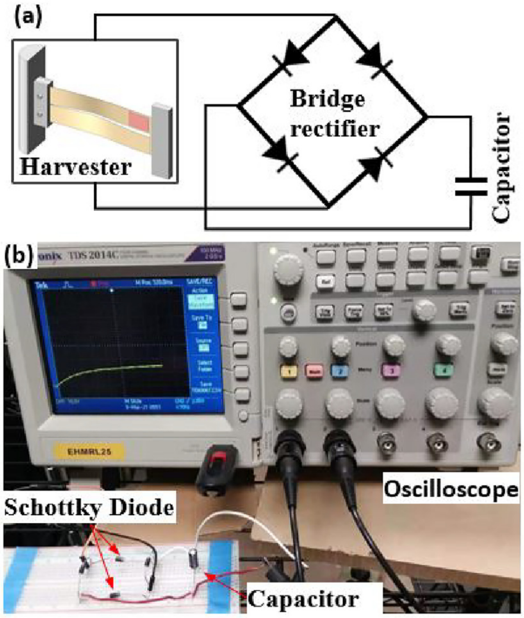

Fig. 10. (a) Diagram of the rectifier circuit and (b) the experimental setup of charging a capacitor.

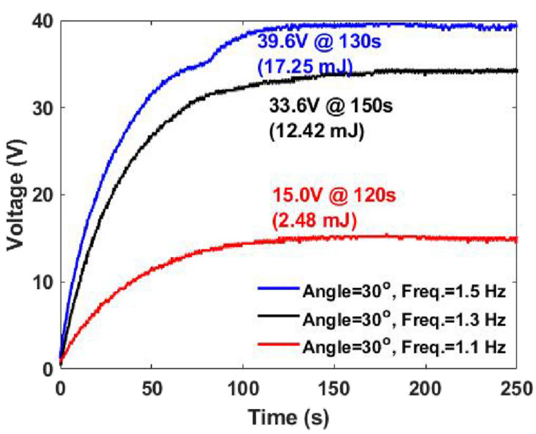

Fig. 11. The process of charging a capacitor of 22 μF.

considered swing frequencies. The capacitor was fully charged, and the current stopped flowing at $V_1 = 15.0$ V, $V_2 = 33.6$ V, $V_3 = 39.6$ V under the swing frequencies of 1.1 Hz, 1.3 Hz, and 1.5 Hz, respectively. The stored energy in the fully charged capacitor can be calculated by

$$E_c = \frac{1}{2} C_c V_f^2 \tag{3}$$

where V_f is the fully charged voltage. Using Eq. (3), it is found that 2.48 mJ, 12.42 mJ, and 17.25 mJ energy was obtained in the capacitor at the three swing frequencies, respectively. The lower voltage and energy in the capacitor at the frequency of 1.1 Hz is imputed to the small-amplitude local vibration of the harvester. More power and higher voltage were achieved by the large-amplitude snap-through oscillations of the harvester at slightly higher swing frequencies of 1.3 Hz and 1.5 Hz. At 1.5 Hz, the charging time took around 130 s to achieve complete charging. These results demonstrate that the proposed bio-inspired bistable piezoelectric energy harvester could provide a sustainable power supply under fish swing motions. More energy could be attained from the snap-through vibrations for intensive data communication.

It's worth noting that this study aims to validate the conceptual design and feasibility of harvesting energy from fish swing and surrounding fluid for self-powered fish tags. There is still much space to improve the design, materials, and system integration in future studies for practical applications. For example, the energy harvesting circuit, energy storage and management, sensing circuit, wireless data transmission, and proper attachment are needed to develop and integrate to enable the self-powered fish tags. The power generation performance of the harvester could be significantly improved by optimization of the parameters. In addition, the nonlinear dynamics of the bistable nonlinear piezoelectric energy harvester under fluid flow is also very interesting to explore theoretically and experimentally in the future. Nevertheless, the current results shed light upon the self-powered animal telemetry tags by harvesting energy from animal motions and surroundings.

6. Conclusion

Inspired by the symbiotic relationship between the remora fish and sharks, a self-powered fish telemetry tag is proposed which includes a novel attachment and a bistable piezoelectric energy harvester. The bistable piezoelectric energy harvester inspired by the bistability of the Venus flytrap leaves is exploited to harvest energy from fish swinging and surrounding fluid. The harvester was tailored from a cantilever beam and curved in two directions by applying a displacement constraint at the free ends of the resultant two sub-beams. A semicircular bluff body was added to the free end of the bistable piezoelectric energy harvester to enhance the fluid-structure interaction to increase power output. The force-displacement curves characterized the bistability of the piezoelectric energy harvester. An experimental setup consisting of a water tank and a servo-drive system was designed to simulate the fish swinging and underwater environment to test the bistable piezoelectric energy harvester. Different swing angles and frequencies, as well as various external resistances, were considered in the experiments. The results demonstrate that the bio-inspired bistable piezoelectric energy harvester could effectively scavenge energy from fish swinging and the surrounding fluid as a sustainable power source for electronic fish tags. The harvester has a much larger power output at properly selected swing angles and frequencies because of the snap-through phenomenon of the bistable harvester. An average power of 1.5 mW was generated at the swing angle of 30^{o} and the frequency of 1.6 Hz.

CRediT authorship contribution statement

Feng Qian: Conceptualization, Methodology, Investigation, Visualization, Supervision, Data curation, Writing – original draft, Writing – review & editing. **Mingyi Liu:** Data curation, Software, Investigation. **Jianuo Huang:** Data curation, Investigation, Visualization. **Jiajun Zhang:** Data curation, Investigation, Visualization. **Hyunjun Jung:** Data curation, Investigation, Visualization. **Zhiqun Daniel Deng:** Supervision, Writing – review & editing, Resources. **Muhammad R. Hajj:** Supervision, Writing – review & editing, Project administration, Resources, Funding acquisition. **Lei Zuo:** Supervision, Writing – review & editing, Project administration, Resources, Funding acquisition.

Declaration of competing interest

The authors declare that they have no known competing financial interests or personal relationships that could have appeared to influence the work reported in this paper.

Acknowledgment

The authors gratefully acknowledge the financial support from the National Science Foundation (Award Numbers: 1935951 and 1935954)

References

[1] R. Kays, S. Tilak, M. Crofoot, T. Fountain, D. Obando, A. Ortega, F. Kuemmeth, J. Mandel, G. Swenson, T. Lambert, et al., Tracking animal location and activity with an automated radio telemetry system in a tropical rainforest, Comput. J. 54 (2011) 1931–1948.

[2] N.E. Hussey, S.T. Kessel, K. Aarestrup, S.J. Cooke, P.D. Cowley, A.T. Fisk, R.G. Harcourt, K.N. Holland, S.J. Iverson, J.F. Kocik, et al., Aquatic animal telemetry: a panoramic window into the underwater world, Science 348 (2015).

[3] D.J. Skerritt, C. Fitzsimmons, N. Polunin, Fine scale acoustic telemetry as an offshore monitoring and research tool recommended practice, Marine Biology, Ecosystems and Governance Research Group, NERC (2015).

[4] J. Lu, Z. Deng, H. Li, M. Myjak, J. Martinez, J. Xiao, R. Brown, S. Cartmell, A small long-life acoustic transmitter for studying the behavior of aquatic animals, Rev. Sci. Instrum. 87 (2016) 114902.

[5] F.A. Voegeli, M.J. Smale, D.M. Webber, Y. Andrade, R.K. O'dor, Ultrasonic telemetry, tracking and automated monitoring technology for sharks, Environ. Biol. Fish. 60 (2001) 267–282.

[6] N. Jepsen, E.B. Thorstad, T. Havn, M.C. Lucas, The use of external electronic tags on fish: an evaluation of tag retention and tagging effects, Animal Biotelemetry 3 (2015) 1–23.

[7] K. Allen, Shark Mitigation and Deterrent Measures Submission 47, Appendix 2 – Overview of Key Concerns Regarding Acoustic Tagging, Parliament of Australia, 2015. URL: https://www.aph.gov.au/DocumentStore.ashx?id=93ddfac1-42ea-4509-9e3f-26feceaf13c9&subId=508725.

[8] M.W. Shafer, E. Morgan, Energy harvesting for marine-wildlife monitoring, in: ASME 2014 Conference on Smart Materials, Adaptive Structures and Intelligent Systems, American Society of Mechanical Engineers Digital Collection, 2014.

[9] W. Sun, D. Zhao, T. Tan, Z. Yan, P. Guo, X. Luo, Low velocity water flow energy harvesting using vortex induced vibration and galloping, Appl. Energy 251 (2019) 113392.

[10] S. Yayla, S. Ayça, M. Oruç, A case study on piezoelectric energy harvesting with using vortex generator plate modeling for fluids, Renew. Energy 157 (2020) 1243–1253.

[11] Y. Gong, X. Shan, H. Hu, T. Xie, Z. Yang, Vortex-induced swing (vis) motion for energy harvesters and flowmeters, Appl. Phys. Lett. 117 (2020) 153904.

[12] C. Zhang, Z. Zhao, O. Yang, W. Yuan, L. Zhou, X. Yin, L. Liu, Y. Li, Z.L. Wang, J. Wang, Bionic-fin-structured triboelectric nanogenerators for undersea energy harvesting, Adv. Mater. Technol. 5 (2020) 2000531.

[13] M.W. Shafer, R. MacCurdy, E. Garcia, Testing of vibrational energy harvesting on flying birds, in: ASME 2013 Conference on Smart Materials, Adaptive Structures and Intelligent Systems, American Society of Mechanical Engineers Digital Collection, 2013.

[14] Y. Cha, M. Verotti, H. Walcott, S.D. Peterson, M. Porfiri, Energy harvesting from the tail beating of a carangiform swimmer using ionic polymer–metal composites, Bioinspiration Biomimetics 8 (2013), 036003.

[15] Y. Cha, W. Chae, H. Kim, H. Walcott, S.D. Peterson, M. Porfiri, Energy harvesting from a piezoelectric biomimetic fish tail, Renew. Energy 86 (2016) 449–458.

[16] A. Erturk, G. Delporte, Underwater thrust and power generation using flexible piezoelectric composites: an experimental investigation toward self-powered swimmer-sensor platforms, Smart Mater. Struct. 20 (2011) 125013.

[17] H. Li, C. Tian, J. Lu, M.J. Myjak, J.J. Martinez, R.S. Brown, Z.D. Deng, An energy harvesting underwater acoustic transmitter for aquatic animals, Sci. Rep. 6 (2016) 1–9.

[18] F. Qian, N. Abaid, L. Zuo, Multiple-scale analysis of a tunable bi-stable piezoelectric energy harvester, ASME.Lett.Dyn.Syst. Control 1 (2021).

[19] E. Fakeih, A.S. Almansouri, J. Kosel, M.I. Younis, K.N. Salama, A wideband magnetic frequency up-converter energy harvester, Adv. Eng. Mater. (2021) 2001364.

[20] K. Fan, Q. Tan, Y. Zhang, S. Liu, M. Cai, Y. Zhu, A monostable piezoelectric energy harvester for broadband low-level excitations, Appl. Phys. Lett. 112 (2018) 123901.

[21] Y. Li, S. Zhou, Z. Yang, T. Guo, X. Mei, High-performance low-frequency bistable vibration energy harvesting plate with tip mass blocks, Energy 180 (2019) 737–750.

[22] H. Fu, E.M. Yeatman, Rotational energy harvesting using bi-stability and frequency up-conversion for low-power sensing applications: theoretical modelling and experimental validation, Mech. Syst. Signal Process. 125 (2019) 229–244.

[23] D. Huang, S. Zhou, Q. Han, G. Litak, Response analysis of the nonlinear vibration energy harvester with an uncertain parameter, Proc. Inst. Mech. Eng. - Part K J. Multi-body Dyn. 234 (2020) 393–407.

[24] H.-X. Zou, W.-M. Zhang, K.-X. Wei, W.-B. Li, Z.-K. Peng, G. Meng, A compressive-mode wideband vibration energy harvester using a combination of bistable and flextensional mechanisms, J. Appl. Mech. 83 (2016).

[25] T. Tan, Z. Yan, K. Ma, F. Liu, L. Zhao, W. Zhang, Nonlinear characterization and performance optimization for broadband bistable energy harvester, Acta Mech. Sin. 36 (2020) 578–591.

[26] F. Qian, S. Zhou, L. Zuo, Approximate solutions and their stability of a broadband piezoelectric energy harvester with a tunable potential function, Commun. Nonlinear Sci. Numer. Simulat. 80 (2020) 104984.

[27] W. Wang, J. Cao, C.R. Bowen, D.J. Inman, J. Lin, Performance enhancement of nonlinear asymmetric bistable energy harvesting from harmonic, random and human motion excitations, Appl. Phys. Lett. 112 (2018) 213903.

[28] C. Lan, W. Qin, Enhancing ability of harvesting energy from random vibration by decreasing the potential barrier of bistable harvester, Mech. Syst. Signal Process. 85 (2017) 71–81.

[29] S. Priya, H.-C. Song, Y. Zhou, R. Varghese, A. Chopra, S.-G. Kim, I. Kanno, L. Wu, D.S. Ha, J. Ryu, et al., A review on piezoelectric energy harvesting: materials, methods, and circuits, Energy Harvesting and Systems 4 (2017) 3–39.

[30] B.E. Flammang, C.P. Kenaley, Remora cranial vein morphology and its functional implications for attachment, Sci. Rep. 7 (2017) 1–5.

[31] R. Masana, M.F. Daqaq, Electromechanical modeling and nonlinear analysis of axially loaded energy harvesters, J. Vib. Acoust. 133 (2011).

[32] S.C. Stanton, C.C. McGehee, B.P. Mann, Nonlinear dynamics for broadband energy harvesting: investigation of a bistable piezoelectric inertial generator, Phys. Nonlinear Phenom. 239 (2010) 640–653.

[33] J. Cao, W. Wang, S. Zhou, D.J. Inman, J. Lin, Nonlinear time-varying potential bistable energy harvesting from human motion, Appl. Phys. Lett. 107 (2015) 143904.

[34] A. Syta, C. Bowen, H. Kim, A. Rysak, G. Litak, Experimental analysis of the dynamical response of energy harvesting devices based on bistable laminated plates, Meccanica 50 (2015) 1961–1970.

[35] D. Pan, F. Dai, Design and analysis of a broadband vibratory energy harvester using bi-stable piezoelectric composite laminate, Energy Convers. Manag. 169 (2018) 149–160.

[36] S.-W. Kim, J.-S. Koh, J.-G. Lee, J. Ryu, M. Cho, K.-J. Cho, Flytrap-inspired robot using structurally integrated actuation based on bistability and a developable surface, Bioinspiration Biomimetics 9 (2014), 036004.

[37] F. Qian, M.R. Hajj, L. Zuo, Bio-inspired bi-stable piezoelectric harvester for broadband vibration energy harvesting, Energy Convers. Manag. 222 (2020) 113174.

[38] R.M. Neville, R.M. Groh, A. Pirrera, M. Schenk, Shape control for experimental continuation, Phys. Rev. Lett. 120 (2018) 254101.

[39] Q. He, M.F. Daqaq, Influence of potential function asymmetries on the performance of nonlinear energy harvesters under white noise, in: International Design Engineering Technical Conferences and Computers and Information in Engineering Conference, vol. 46391, American Society of Mechanical Engineers, 2014. V006T10A060.

[40] J.B. Graham, H. Dewar, N. Lai, W.R. Lowell, S.M. Arce, Aspects of shark swimming performance determined using a large water tunnel, J. Exp. Biol. 151 (1990) 175–192.

[41] Y. Liao, H.A. Sodano, Optimal parameters and power characteristics of piezoelectric energy harvesters with an rc circuit, Smart Mater. Struct. 18 (2009), 045011.